Journal of Chemical&Engineering Data

pubs.acs.org/jced

Article

Competitive Adsorption of Vanillin, Vanillic Acid, and Acetovanillone onto SP700 Resin

Albertina G. Rios, Carina A. E. Costa,* Ana M. Ribeiro, Alírio E. Rodrigues, and Alexandre F. P. Ferreira

Cite This: *J. Chem. Eng. Data* 2024, 69, 3660−3667

ABSTRACT: In this work, the recovery of phenolic monomers obtained from the oxidative depolymerization of lignin was studied. The adsorption of aromatic aldehydes, acids, and ketones using a macroporous polymeric resin, Sepabeads SP700, was assessed experimentally. Batch experiments were performed by using aqueous model solutions for each phenolic monomer. The adsorption equilibrium for vanillin, vanillic acid, and acetovanillone in single-component and ternary mixtures was evaluated. Experimental results were regressed against the Bi-Langmuir model. The validity of a phenomenological model, comprising the adsorption equilibrium isotherm model and the linear driving force approximation for particle mass transfer, was confirmed through experimental validation using fixed bed dynamic adsorption tests. For a ternary mixture with V concentration of 4 g·L^{-1}, VA of 0.8 g·L^{-1}, and VO of 0.08 g·L^{-1}, the adsorbed amounts are 0.57 g·g$^{-1}_{\text{dry resin}}$, 0.05 g·g$^{-1}_{\text{dry resin}}$, and 0.02 g·g$^{-1}_{\text{dry resin}}$, respectively. This work is the first step toward the implementation of the ternary separation in a pseudo-SMB (JO-process).

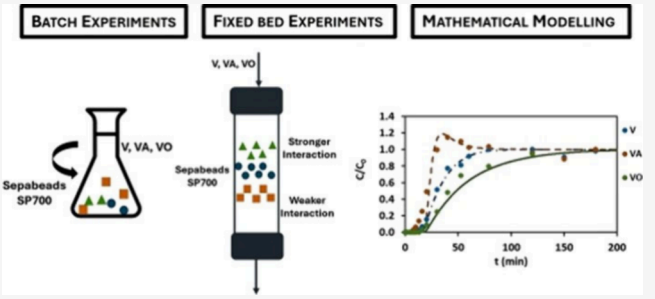

1. INTRODUCTION

Lignin is one of the most important components of side streams from lignocellulosic-based biorefineries and the pulp and paper industries. This three-dimensional biopolymer is produced worldwide in amounts close to 70 million tonnes per year, and only 2% is used as a precursor for chemicals and materials production.[1] Consequently, producing valuable phenolic compounds from lignin, a renewable source, emerges as a promising alternative to explore its potential. Lignin depolymerization through alkaline oxidation, at controlled conditions, is one of the possible valorization routes, giving origin to a complex mixture of products containing lignin oligomers, dimers, low-molecular-weight phenolic monomers, and minor amounts of other secondary nonphenolic compounds.[2] Therefore, the effective and specific separation of aromatic compounds of interest is still one of the most important obstacles to their production from lignin. These compounds are usually difunctional and include aromatic aldehydes (i.e., vanillin and syringaldehyde), their respective aromatic acids (vanillic and syringic acids), and ketones (acetovanillone and acetosyringone), whose selectivity and efficiency depend strongly on processing conditions, lignin origin, and oxidation conditions.[3,4] The similarity between the physicochemical properties of these aromatic monomers (i.e., their molecular weights, acid dissociation constants, densities, and boiling points—see Table 1) is a challenge considering their separation from the oxidized lignin mixture and their consequent purification process.[5]

Table 1. Physicochemical Properties of Vanillin, Vanillic Acid, and Acetovanillone

Compound	Vanillin	Vanillic acid	Acetovanillone
Molecular formula	$C_8H_8O_3$	$C_8H_8O_4$	$C_9H_{10}O_3$
Structure			
Molecular weight, g/mol	152.15	168.15	166.17
Density, g/cm^3	1.06	1.40	1.17
Boiling point, °C	285	257	264
Water solubility, g/L (25°C)	10.0	1.3	< 1.0
*p*Ka	7.4	4.5	8.2

Research on separation and purification processes has gained special attention due to the demand for greener and lower-impact methodologies to obtain rich fractions of valuable compounds from dilute solutions. Adsorption, with its relative simplicity of design, operation, scale-up, versatility, low cost, and high efficiency, has aroused great interest in the selective separation of phenolic compounds.[6,7] Regarding the typical

Special Issue: In Honor of Maria Eugenia Macedo

Received: April 11, 2024
Revised: July 22, 2024
Accepted: August 2, 2024
Published: August 13, 2024

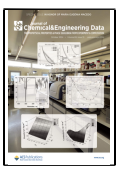

Table 2. IUPAC Name, CAS Registry Number, and Purity of the Chemicals Used

Compound	IUPAC name	CAS Reg. No.	Purity (m%)[a]
Vanillin	4-Hydroxy-3-methoxybenzaldehyde	121−33−5	≥97%
Vanillic acid	4-Hydroxy-3-methoxybenzoic acid	121−34−6	≥98%
Acetovanillone	1-(4-Hydroxy-3-methoxyphenyl)ethanone	498−02−2	≥98%

[a]m% refers to mass percentage.

phenolic monomers found in lignin-oxidized medium, their separation remains a challenge since most of the studies available in the literature only evaluate their recovery from model solutions, and studies performed with real mixtures are scarcer. Töppel reported the first study about vanillin adsorption in a patent from 1959, where it attempted to improve the adsorption of aldehydes and ketones using a polystyrene sulfonic acidic cation-exchange resin.[8] However, polymeric resins have attracted the most interest in the recovery of phenolic monomers from different media.[5,9−12] The existence of both hydrophobic and hydrophilic groups in the resin molecule, the possibility of constant pH along the process, the chemical stability and inert nature, the ability to simultaneously recover phenolics and regenerate the resin in a single step, and the modeling of their adsorptive properties based on surface hydrophobicity, surface area, and porosity have a great influence on its adsorption performance in a varied range of conditions.[13] Mota and co-workers have studied the purification of an oxidized industrial kraft liquor containing different families of phenolic compounds by chromatographic processes using SP700 resin.[7] The authors observed that vanillic and syringic acids are practically not adsorbed onto the resin, and their separation from the respective ketones (acetovanillone and acetosyringone) and aldehydes (vanillin and syringaldehyde) can be accomplished. In another work, Wu and co-workers stated that the resin X-5 has higher adsorption rates of *p*-hydroxybenzaldehyde, vanillin, and syringaldehyde than those of CAD-40, D101, and AB-8 resins due to its nonpolarity and larger surface area that was more likely to adsorb lignin-based aromatic aldehydes.[14] Besides the studies that proved the effectiveness of polymeric resins for phenolic monomer separation, the influence of the most important operational variables on the recovery process through adsorption should also be evaluated. Temperature and pH are key factors determining the adsorption efficiency when employing polymeric resins.[6] At acidic pH, the adsorptive capacity of the polymeric resins for phenolic compounds is enhanced because the phenols are undissociated and the dispersion interactions are predominant. At alkaline pH, adsorption decreases since dissociation of hydroxyl groups and carbonyl groups occurs, and the ionized compound fraction becomes more relevant and is not adsorbed.[6,15] Temperature also influences adsorption through the increase of the transport rate across the external boundary layer and within the pores due to the decreased solution viscosity and, on the other hand, by reducing the adsorption capacity of the adsorbent.[16] Moreover, high temperatures may promote irreversible interactions.[17]

The main challenge of employing polymeric adsorbents for the separation of different families of phenolic monomers from oxidation solutions from lignin depolymerization will be the lack of selectivity for the target compounds due to their physicochemical similarities, and consequently, further purification processes are required to obtain a commercially high purity product. Moreover, several limitations must be overcome before an adsorption−desorption process can be scaled up, such as eluent cost, adsorption loss, and the regeneration of the stationary phase. This work studies the competitive adsorption behaviors of vanillin, vanillic acid, and an acetovanillone mixture on macroporous polymeric adsorbent-rein Sepabeads SP700. Batch adsorption isotherms of vanillin, acid vanillic, and acetovanillone in single- and ternary-component systems in aqueous solution were assessed, obtaining the respective equilibrium isotherms. Fixed bed studies were also performed to validate the mathematical model obtained, and the potential of the separation process of the phenolic monomers studied was evaluated.

2. EXPERIMENTAL AND COMPUTATIONAL METHODS

2.1. Chemicals and Adsorbent. All of the phenolic monomers studied in the adsorption experiments of this work, vanillin (V), vanillic acid (VA), and acetovanillone (VO), were purchased from Sigma-Aldrich. The IUPAC name, CAS registry number, and purity of each chemical are listed in Table 2.

The adsorption experiments were performed with aqueous model solutions of the phenolic monomers using a styrene-divinylbenzene-based synthetic adsorbent, Sepabeads SP700 (Mitsubishi Chemical Corporation). A description of the physical and chemical properties of the resin Sepabeads SP700 can be found in Table 5 of this manuscript.

2.2. Analytical Method. The phenolic monomer concentration was evaluated by high-performance liquid chromatography with ultraviolet detection (HPLC-UV), employing a Knauer HPLC system (Germany) with a Smartline 5000 online degasser, a Smartline 1000 quaternary pump, and a Smartline 2600 UV − DAD operating at 280 nm. An analytical reversed-phase column ACE 5 C18-pentafluorophenyl group (250 × 3.0 mm, 5 μm) with a guard column of the same material was used for the analyses. Two eluents were used: water/methanol 95%/5% (v/v) and water/methanol 5%/95% (v/v), both acidified with formic acid (0.1%). Further detailed information about the equipment and conditions is described elsewhere.[18,19]

2.3. Resin Activation. The adsorbent, SP700 resin, was activated by performing a sequence of steps using different solutions of water and methanol. A detailed activation procedure has already been described in the literature.[9]

2.4. Batch Adsorption Equilibrium Isotherms. Batch adsorption experiments were conducted with monocomponent aqueous model solutions of V, VA, and VO. The experiments were performed with 50 mL of each model solution containing 4 g·L^{-1} of V, 0.8 g·L^{-1} of VA, and 0.08 g·L^{-1} of VO. Different amounts of SP700 resin were used, ranging from 0.025 to 1.75 g of dry basis weight. Batch samples were equilibrated at 25 °C and 200 rpm, on a shaking incubator (Jeiotech SI-300) for 24 h in the case of VA and 48 h for V and VO, to ensure the equilibrium was reached and there was no degradation of the phenolic monomers.

https://doi.org/10.1021/acs.jced.4c00193
J. Chem. Eng. Data 2024, 69, 3660−3667

Multicomponent mixtures were used to obtain equilibrium data points, initially with the same concentrations as the single-component experiments (V = 4g/L, VA = 0.8 g/L, and VO = 0.08 g/L) and using different dry adsorbent masses (0.5 0.2, and 0.05 g). Additionally, another set of experiments was conducted with an initial concentration of 0.7 g·L^{-1} of V, 0.6 g·L^{-1} of VA, and 0.3 g·L^{-1} of VO, using 0.6 g, 0.3 g, 0.1 g, and 0.05 g of dry resin. Finally, a binary mixture with 0.8 g·L^{-1} of VA and 0.08 g·L^{-1} of VO was also used to obtain binary equilibrium points, using 0.5, 0.2, and 0.05 g of dry resin. The initial pH of the solutions was measured, and it was 4.3, 3.3, and 5.3 for the V, VA, and VO, respectively. Also, no pH adjustments were made to the phenolic monomer solutions. After adsorption, no significant changes in this parameter were noticed.

The dry adsorbent mass was obtained based on a coefficient ratio of dry and wet adsorbent mass, f_h.

Therefore, the initial feed concentration and equilibrium concentrations of V, VA, and VO were quantified by HPLC-UV, as described in section 2.2.

The adsorption capacity of the adsorbent for each phenolic monomer studied is estimated through a material mass balance between the adsorbent and the liquid phase using equation 1

$$q_{e,i} = \frac{(C_{0,i} - C_{e,i})V}{m_{\text{ads}}} \tag{1}$$

where q_e is the adsorbed phase equilibrium concentration; C_0 represents the initial concentration of adsorbate of the solution; C_e is the adsorbate equilibrium concentration of the supernatant solution; V is the initial volume solution; m_{ads} is the dry weight of the adsorbent, and i is the phenolic species studied.

2.5. Fixed Bed Adsorption Studies. The resin SP700 was packed in a jacketed glass column (Götec, Germany) with an 8.5 cm length and 1 cm internal diameter for the studies of fixed bed adsorption. Aqueous V, VA, and VO solutions were fed to the column with a Smartline Pump 1000 (Knauer, Germany), and isothermal conditions were assured with a thermostatic water bath (Lauda). Experiments were performed at 25 °C and feed concentrations of 4.0, 0.8, and 0.08 g·L^{-1} for V, VA, and VO, respectively, at a fixed flow rate (approximately 5 mL·min^{-1}). Breakthrough curves were obtained for the three compounds in monocomponents and in ternary mixtures. Column regeneration was performed using a solution with 50%/50% ethanol/water.

Preliminary tests were conducted to assess the packing-related parameters. The bed porosity ε_b was measured by a tracer experiment using blue dextran.

2.6. Adsorption Equilibrium Isotherms. The Bi-Langmuir model was proposed to describe the adsorption equilibrium data obtained for V, VA, and VO in an aqueous solution onto SP700 resin. This model considers two different sites for adsorption, and each site behaves independently, following Langmuir principles.

$$q_{e,i} = \frac{Q_{m1,i}K_{L1,i}C_{i,e}}{1 + K_{L1,i}C_{i,e}} + \frac{Q_{m2,i}K_{L2,i}C_{i,e}}{1 + K_{L2,i}C_{i,e}} \tag{2}$$

where Q_{m1} and Q_{m2} are the two maximum adsorption capacities, and K_{L1} and K_{L2} are the Langmuir equilibrium constants related to the free energy for adsorption.

The extended Bi-Langmuir model described the adsorption equilibrium in a ternary mixture of V, VA, and VO. This model considers that all sites are equivalent and each site holds one molecule.

$$q_{e,i} = \frac{Q_{m1,i}K_{L1,i}C_{i,e}}{1 + \sum_{j=1}^{NC} K_{L1,j}C_{j,e}} + \frac{Q_{m2,i}K_{L2,i}C_{i,e}}{1 + \sum_{j=1}^{NC} K_{L2,j}C_{j,e}} \tag{3}$$

The parameter estimation considers both single and ternary mixture adsorption equilibrium isotherms.

2.7. Fixed Bed Model. The mathematical model that describes the breakthrough curves of the phenolic compounds assumes isothermal operation, plug flow with axial dispersion, constant bed voidage, and no radial gradients within the bed. The mass balance included in the fluid phase in a bed volume element is described by the following equation:

$$\frac{\partial C_{bi}}{\partial t} = D_{ax}\frac{\partial^2 C_{bi}}{\partial z^2} - u_i\frac{\partial C_{bi}}{\partial z} - \frac{(1 - \varepsilon_b)}{\varepsilon_b}f_h\rho_p\frac{\partial \overline{q}_i}{\partial t} \tag{4}$$

where C_b is the bulk concentration; $\overline{q}$ is the average adsorbed phase concentration; Z is the axial column dimension; ε_b is the bed porosity; u_i is the interstitial velocity; D_{ax} is the axial dispersion coefficient; f_h is the mass of dry particle to mass of wet particle ratio; ρ_p is the wet particle density; and t is the time.

The linear driving force (LDF) equation describes the particle's mass balance.

$$\frac{\partial \overline{q}_i}{\partial t} = k_{h,i}(q_{e,i} - \overline{q}_i) \tag{5}$$

where k_h is the mass transfer coefficient.

Initial conditions for each column:

$$t = 0 \rightarrow C_{bi} = q_i = 0 \tag{6}$$

The following equations describe the boundary conditions:

$$u_i C_{bi}^{\text{in}} = u_i C_{bi}|_{z=0} - D_{ax}\left.\frac{\partial C_{bi}}{\partial z}\right|_{z=0} \tag{7}$$

$$\left.\frac{\partial C_{bi}}{\partial z}\right|_{z=L} = 0 \tag{8}$$

The axial dispersion in the packed bed was estimated based on the Peclet number obtained experimentally and using the following equation:

$$Pe_L = \frac{u_i L}{D_{ax}} \tag{9}$$

The mass transfer coefficient was estimated considering the homogeneous particle and calculated based on equation 10.

$$k_{h,i} = \frac{15D_{pe,i}}{R_p^2 f_h \rho_b \frac{dq_{e,i}}{dC_{e,i}}} \tag{10}$$

where R_p is the particle radius and $\frac{dq_{e,i}}{dC_{e,i}}$ is the slope of the adsorption equilibrium isotherm.

The effective pore diffusivity is estimated from the following equations:[20]

$$D_{p,i} = \frac{\varepsilon_p D_{m,i}}{\tau} \tag{11}$$

https://doi.org/10.1021/acs.jced.4c00193
J. Chem. Eng. Data 2024, 69, 3660−3667

where τ is the tortuosity, $\tau = \frac{2-\varepsilon_p}{\varepsilon_p}$, and D_m is the molecular diffusivity.

The molecular diffusivity, D_m is estimated by the Wilke–Chang correlation:[21]

$$D_{m,i} = 7.4 \times 10^{-10} \frac{T\sqrt{\phi M}}{\mu V_m^{0.6}} \quad (12)$$

where T is the absolute temperature; ϕ is the association factor, which is considered 2.6 for water; M is the molecular weight of the solvent; μ is the viscosity of the solvent; and V_m is the molar volume of solute at its normal boiling point.

Based on the material mass balance, the mathematical model was solved using the gPROMS software (general PROcess Modeling System). Simulations were conducted by discretizing the axial coordinate using the orthogonal collocation in finite elements method (OCFEM) with second-order polynomials. A total of 40 finite elements were utilized. To solve the system of ordinary differential and algebraic equations that resulted from the discretization process, the DAEBDF solver was utilized with an absolute tolerance of 10^{-6}.

3. RESULTS AND DISCUSSION

3.1. Adsorption Equilibrium Isotherms. The adsorption equilibrium of V, VA, and VO was measured in an aqueous solution onto a Sepabeads SP700 resin. The equilibrium was fitted with the Bi-Langmuir model, so that one can predict ternary adsorption equilibrium. The adsorption equilibrium data and experimental and model results for the single-component adsorption equilibrium isotherms are shown in Figure 1, Figure 2, and Figure 3. The experimental points are reported in Table S.1 of the Supporting Information.

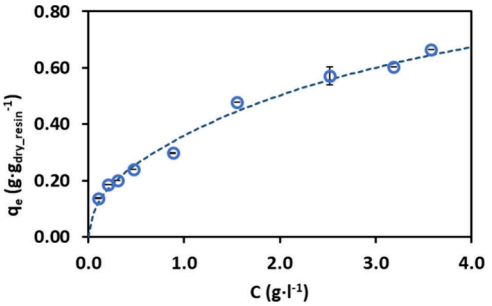

Figure 1. Adsorption equilibrium isotherm for V in water onto the adsorbent Sepabeads SP700 at 25 °C. The points represent experimental data, and the dashed line (--) is the Bi-Langmuir model.

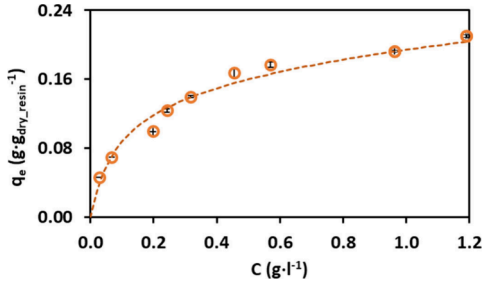

Figure 2. Adsorption equilibrium isotherm for VA in water onto the adsorbent Sepabeads SP700 at 25 °C. The points represent experimental data, and the dashed line (--) is the Bi-Langmuir model.

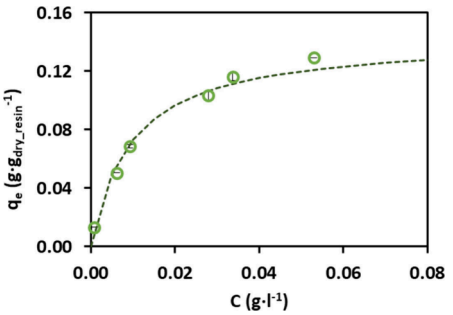

Figure 3. Adsorption equilibrium isotherm for VO in water onto the adsorbent Sepabeads SP700 at 25 °C. The points represent experimental data, and the dashed line (--) is the Bi-Langmuir model.

As observed from the data, V demonstrates a higher adsorption capacity within the selected concentration range for each phenolic compound compared with VA and VO, as illustrated by the overlaid isotherms in Figure 4 (a). Therefore, this discrepancy can be attributed to the constraint imposed by the water solubility of each compound, which was approximately 10 g·L^{-1} for V and 1.3 g·L^{-1} for VA, while for VO, its solubility in cold water is very low, with a value <0.1 g·L^{-1}.[18]

At lower concentrations (below 0.1 g·L^{-1}) of all components, VO demonstrates higher adsorbed amounts than the other two phenolic compounds, as illustrated in Figure 4, where the adsorption equilibrium isotherms for all three monomers are overlaid. This trend becomes more pronounced in Figure 4 (b), in which zoom-ins on the concentration range of 0.00–0.25 g·L^{-1} are showed.

In this work, the Bi-Langmuir isotherm was deemed the most suitable model to fit the experimental data from the multicomponent adsorption equilibrium experiment using the aqueous ternary mixture of V, VA, and VO. This model had been previously applied to fit equilibrium data from batch experiments of vanillic and syringic acids in water, and the adsorption of these phenolic acids onto Sepabeads SP700 resin was studied.[22] Moreover, both Langmuir and Freundlich isotherms have been used in previous studies for the adsorption of vanillin and syringaldehyde, as documented in the literature.[5,9,23] The multicomponent adsorption equilibrium of V, VA, and VO was achieved under the same conditions as those for the single-component equilibrium points. Different initial concentrations were used as reported in section 2.4.

Table 3 reports the experimental data for the multicomponent points for the adsorption equilibrium, alongside the predictions obtained by the extended multicomponent equation. The results are divided into three groups, and a total of 10 equilibrium points were obtained: three points 1.1–1.3 (a ternary mixture with initial concentration of 2 g·L^{-1} of V, 0.8 g·L^{-1} of VA, and 0.08 g·L^{-1} of VO), four points of the other ternary mixture, 2.1–2.4 (initial concentrations of 0.7 g·L^{-1} of V, 0.6 g·L^{-1} of VA, and 0.3 g·L^{-1} of VO), and binary mixture, 3.1–3.3 (with an initial concentration of 0.8 g·L^{-1} of VA and 0.08 g·L^{-1} of VO).

All of the experimental points and the respective error are reported in Table S.2 of the Supporting Information. Also, is given a prediction by the Ideal Adsorption Solution Theory (IAST) is given in Table S.4 and Figure S1.

In Table 4, the adsorption equilibrium parameters are reported. As the main objective of this work is to obtain a mathematical model that considers the competitive adsorption

https://doi.org/10.1021/acs.jced.4c00193
J. Chem. Eng. Data 2024, 69, 3660–3667

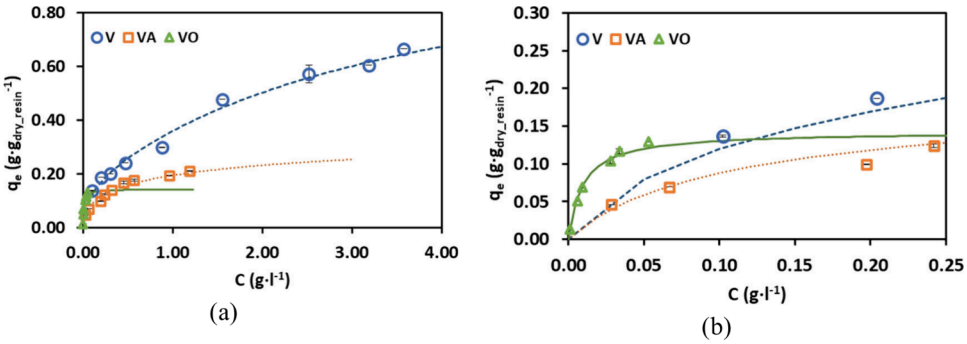

Figure 4. Adsorption equilibrium isotherms for V, VA, and VO in water onto the adsorbent Sepabeads SP700 at 25 °C. The points represent experimental data, and the lines represent the Bi-Langmuir model.

Table 3. Adsorption Equilibrium Isotherm for Multicomponent Mixtures of V, VA, and VO in Water onto the Adsorbent Sepabeads SP700 at 25 °C

	Experimental data						Model data Bi-Langmuir		
Points	C_V (g/L)	C_{VA} (g/L)	C_{VO} (g/L)	q_V (g/g)	q_{VA} (g/g)	q_{VO} (g/g)	q_V (g/g)	q_{VA} (g/g)	q_{VO} (g/g)
1.1	1.155	0.395	0.017	0.296 ± 0.002	0.038 ± 0.000	0.007 ± 0.000	0.324	0.053	0.011
1.2	2.501	0.572	0.040	0.401 ± 0.037	0.051 ± 0.010	0.012 ± 0.000	0.476	0.047	0.013
1.3	3.512	0.726	0.070	0.584 ± 0.121	0.049 ± 0.022	0.018 ± 0.001	0.547	0.048	0.016
2.1	0.036	0.090	0.014	0.054 ± 0.000	0.041 ± 0.000	0.023 ± 0.000	0.033	0.049	0.052
2.2	0.140	0.227	0.041	0.090 ± 0.000	0.058 ± 0.000	0.041 ± 0.000	0.068	0.058	0.062
2.3	0.424	0.463	0.142	0.138 ± 0.000	0.061 ± 0.004	0.076 ± 0.002	0.119	0.059	0.079
2.4	0.516	0.495	0.188	0.168 ± 0.037	0.083 ± 0.037	0.097 ± 0.016	0.133	0.056	0.084
3.1	-	0.038	0.001	-	0.057 ± 0.000	0.007 ± 0.000	0.000	0.048	0.014
3.2	-	0.516	0.031	-	0.083 ± 0.000	0.039 ± 0.000	0.000	0.126	0.046
3.3	-	0.578	0.052	-	0.069 ± 0.000	0.053 ± 0.000	0.000	0.118	0.059

Table 4. Model Equilibrium Parameters Obtained for V, VA, and VO Adsorption onto Sepabeads SP700 Resin

	V	VA	VO
Q_{m1} (g·g$^{-1}_{dry\ resin}$)	1.10	0.13	-
K_{L1} (L·g^{-1})	0.20	0.33	-
Q_{m2} (g·g$^{-1}_{dry\ resin}$)	0.20	0.16	0.15
K_{L2} (L·g^{-1})	12.0	11.7	103

Table 5. Bed Characteristics and Adsorbent Properties

Column with SP700 resin	
pore radius (Å)	90
specific surface area (m^2·g^{-1})	1200
ε_b	0.46
ρ_p (g$_{wet\ resin}$·L$^{-1}_{wet\ resin}$)	1.01
d_p (m)	4.5×10^{-4}
ε_p	0.73
V_c (cm^3)	6.7
m_{ads} (g)	1.3
f_h (g$_{dry\ resin}$·g$^{-1}_{wet\ resin}$)	0.33

of the three studied phenolic monomers, it was necessary to consider the ternary mixture points to obtain the equilibrium parameters.

From the ternary adsorption data, it is observed that the adsorbed amounts of V, VA, and VO all decrease on the resin SP700 in a ternary mixture. Therefore, the adsorbed amount of V is only slightly lower in a ternary mixture compared with a single-component solution. However, the adsorbed amounts of the other two phenolic compounds, VA and VO, decrease considerably when present in the ternary mixture. This suggests a competitive interaction among the three compounds, a phenomenon effectively described by the adsorption equilibrium model presented in Table 3.

The maximum adsorption capacity values for V and VA align with those reported in the literature.[9,22,24] For VO, there is a lack of available adsorption data in the literature, which makes it difficult to make a meaningful comparison.

3.2. Fixed Bed Adsorption Experiments. In the fixed bed experiments, the first stage involves the characterization of the adsorption bed, focusing on both the adsorbent and packing procedure. These crucial parameters are detailed in Table 5.

The bed porosity was assessed by using the blue dextran tracer method. The particle porosity was obtained from prior work that used the same adsorbent and applied helium pycnometry and mercury intrusion techniques.[9] The particle dry mass to wet mass ratio, f_h, was obtained by drying the adsorbent at 60 °C during 12 h. The moisture content of the adsorbent was 67%.

Breakthrough curves were acquired by following the methodology described previously in section 2.5. The parameters used in the fixed bed adsorption model are outlined in Table 6. The particle diameter used in the model was 4.5×10^{-4} m as detailed in Table 5. The axial dispersion parameter was estimated using the Peclet number and considering a flow rate of 2.5 mL·min^{-1}. The mass transfer coefficient was initially estimated using the aforementioned correlations. Subsequently, actual values were determined from the experimental data collected.

A mathematical model was employed to describe the dynamic adsorption behavior for all breakthrough experiments.

https://doi.org/10.1021/acs.jced.4c00193
J. Chem. Eng. Data 2024, 69, 3660−3667

Table 6. Model Mass Transport Parameters

	V	VA	VO
D_{ax} ($m^2 \cdot s^{-1}$)		1.01×10^{-5}	
D_m ($m^2 \cdot s^{-1}$)	7.86×10^{-10}	7.66×10^{-10}	7.30×10^{-10}
D_{pe} ($m^2 \cdot s^{-1}$)	2.60×10^{-10}	2.53×10^{-10}	2.41×10^{-10}
k_h (s^{-1})	1.0×10^{-3}	1.0×10^{-3}	1.4×10^{-3}

Figure 5, Figure 6, and Figure 7 present the fixed bed experiments for the adsorption of V, VA, and VO, respectively.

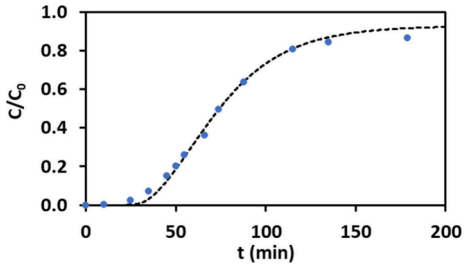

Figure 5. Normalized concentration of V versus time at the adsorption outlet. Conditions: Feed concentration of 4 $g \cdot L^{-1}$ onto the Sepabeads SP700 resin at 25 °C and flow rate of 2.5 $mL \cdot min^{-1}$. Points correspond to the experimental data, and the line corresponds to the Bi-Langmuir mathematical model.

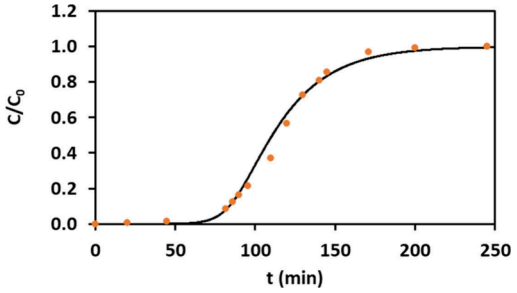

Figure 6. Normalized concentration of VA versus time at the adsorption outlet. Conditions: Feed concentration of 0.8 $g \cdot L^{-1}$ was added onto the Sepabeads SP700 resin at 25 °C and flow rate of 2.5 $mL \cdot min^{-1}$. Points correspond to the experimental data and the line to the Bi-Langmuir mathematical model.

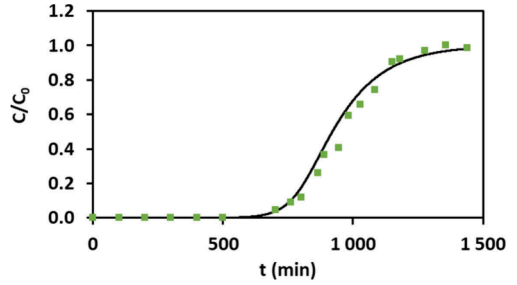

Figure 7. Normalized concentration of VO versus time at the adsorption outlet. Conditions: Feed concentration of 0.08 $g \cdot L^{-1}$ onto the Sepabeads SP700 resin at 25 °C and flow rate of 2.5 $mL \cdot min^{-1}$. Points correspond to the experimental data, and the line to the Bi-Langmuir mathematical model.

All of the experiments were conducted using a flow rate of 2.5 $mL \cdot min^{-1}$. The column was regenerated between experiments using a 50%/50% ethanol/water mixture. The experimental data points are reported in Tables S.5, S.6, and S.7 of the Supporting Information.

Table 7 presents the results for the V, VA, and VO single-component breakthrough curves. The stoichiometric time and

Table 7. Experimental Conditions, Stoichiometric Time, and Adsorption Capacity for V, VA, and VO for Single-Component Data

Solute	V	VA	VO
C^F ($g \cdot L^{-1}$)	4	0.8	0.08
Q ($mL \cdot min^{-1}$)		2.5	
t_{st} (min)	83	121	885
q_e ($g \cdot g^{-1}_{dry\ resin}$)[a]	0.71	0.19	0.12
q^a ($g \cdot g^{-1}_{dry\ resin}$)	0.72	0.18	0.13
SD[b] (%)	1.1	0.4	0.2

[a]The q_e is the adsorbed amount from the single-component adsorption equilibrium isotherm (batch). [b]SD corresponds to the standard deviation between the experimental and theoretical adsorbed amounts calculated with the following expression: $\mathrm{SD}\ (\%) = \sqrt{\frac{(q_{model} - q_{exp})^2}{2}} \times 100$.

the experimentally adsorbed amount were calculated based on the adsorption step. The adsorbed amount was estimated using eq 13.

$$q^* = \frac{C^F Q t_{st} - \varepsilon_b V_c C^F}{m_{ads}} \tag{13}$$

where C^F is the feed concentration at column inlet; Q is the flow rate; t_{st} is the stoichiometric time; and V_c the column volume.

The following expression determined the stoichiometric time:

$$t_{st} = \int_0^\infty \left(1 - \frac{C}{C^F}\right) dt \tag{14}$$

where C is the solute concentration at the column outlet for time t. This value is obtained based on the area underneath the $1 - \frac{C}{C^F}$ line.

It also presents the predicted adsorbed amount based on the adsorption equilibrium isotherm. The Bi-Langmuir model accurately predicted the adsorption data, with the standard deviation error between the experimental and predicted adsorbed amounts being less than 10% for the three phenolic monomers studied. Additionally, concerning the stoichiometric times at the same flow rate, the compound with the least retention in the column is V, while the compound with the highest retention is VO.

Figure 8 presents a ternary breakthrough curve, showing both experimental and model results using the same feed concentrations as those used in the single-component breakthrough curves.

The prediction of the ternary breakthrough curve was obtained based on the adsorption equilibrium data. The model agrees with the experimental results as the error in the adsorbed amounts is lower than 10%. The results regarding the ternary breakthrough curve are presented in Table 8.

The adsorbed amounts for the three phenolic monomers are lower in the ternary mixture compared to those in the single-component experiments, as previously noted from the adsorption equilibrium data. Additionally, due to the competition, the stoichiometric times do not align with those observed in the single-component tests; notably, in the ternary

https://doi.org/10.1021/acs.jced.4c00193
J. Chem. Eng. Data 2024, 69, 3660−3667

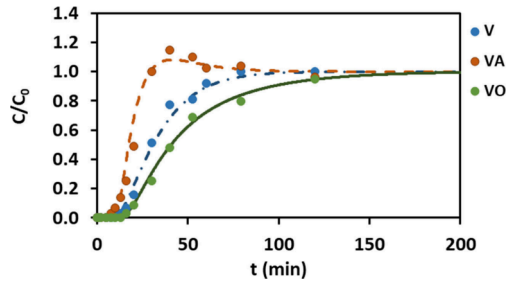

Figure 8. Normalized concentration of V, VA, and VO versus time at the adsorption outlet. Conditions: Feed concentration of 4 g·L^{-1} for V, 0.8 g·L^{-1} for VA, and 0.08 g·L^{-1} for VO onto the Sepabeads SP700 resin at 25 °C and flow rate of 5.0 mL min^{-1}. Ternary breakthrough curve: points correspond to the experimental data and lines to the extended Bi-Langmuir mathematical model.

Table 8. Experimental Conditions, Stoichiometric Time, and Adsorption Capacity for the Ternary Breakthrough Curve

	Ternary		
Solute	V	VA	VO
C^F (g·L^{-1})	4	0.8	0.08
Q (mL·min^{-1})		5.0	
q_e (g·g$^{-1}_{\text{dry resin}}$)	0.57	0.047	0.02
q^a (g·g$^{-1}_{\text{dry resin}}$)^a	0.62 (0.70)	0.05 (0.18)	0.02 (0.13)
SD (%)	3.6	0.5	0.2

^{a}In parentheses are the data relating to the single-component experiments.

mixture, V presents a 17% lower adsorbed amount when compared to single-component adsorption. In contrast, VA and VO demonstrate significantly reduced adsorbed amounts, with losses of 72% and 84% in adsorption in a ternary mixture, respectively.

These experiments were performed to validate the previously described mathematical model and to understand the potential of this resin for separating these three phenolic compounds obtained from lignin oxidative depolymerization.

4. CONCLUSIONS

Adsorption studies of vanillin, vanillic acid, and acetovanillone were performed using a macroporous adsorbent, Sepabeads resin SP700. Adsorption equilibrium isotherms in aqueous solutions were established for the three phenolics individually and for ternary mixtures. The experimental data were fitted by using the Bi-Langmuir model. These experiments revealed the presence of competition among the adsorbates, which the adsorption equilibrium model characterizes.

Fixed bed experiments were also performed on a jacketed column. These experiments utilized the same conditions of temperature and concentration as the batch experiments for generating breakthrough curves. A mathematical model comprising the adsorption equilibrium isotherm and LDF approximation to represent the intraparticle mass transfer was used and validated with single and ternary breakthrough experiments.

ASSOCIATED CONTENT

Supporting Information

The Supporting Information is available free of charge at https://pubs.acs.org/doi/10.1021/acs.jced.4c00193.

Measured data of adsorption equilibrium isotherms and fixed bed experiments (PDF)

AUTHOR INFORMATION

Corresponding Author

Carina A. E. Costa − *LSRE-LCM − Laboratory of Separation and Reaction Engineering - Laboratory of Catalysis and Materials, Faculty of Engineering and ALiCE − Associate Laboratory in Chemical Engineering, Faculty of Engineering, University of Porto, 4200-465 Porto, Portugal;* orcid.org/0000-0001-5136-3803; Email: carina.costa@fe.up.pt

Authors

Albertina G. Rios − *LSRE-LCM − Laboratory of Separation and Reaction Engineering - Laboratory of Catalysis and Materials, Faculty of Engineering and ALiCE − Associate Laboratory in Chemical Engineering, Faculty of Engineering, University of Porto, 4200-465 Porto, Portugal;* orcid.org/0000-0002-9834-1334

Ana M. Ribeiro − *LSRE-LCM − Laboratory of Separation and Reaction Engineering - Laboratory of Catalysis and Materials, Faculty of Engineering and ALiCE − Associate Laboratory in Chemical Engineering, Faculty of Engineering, University of Porto, 4200-465 Porto, Portugal;* orcid.org/0000-0003-4269-1420

Alírio E. Rodrigues − *LSRE-LCM − Laboratory of Separation and Reaction Engineering - Laboratory of Catalysis and Materials, Faculty of Engineering and ALiCE − Associate Laboratory in Chemical Engineering, Faculty of Engineering, University of Porto, 4200-465 Porto, Portugal;* orcid.org/0000-0002-0715-4761

Alexandre F. P. Ferreira − *LSRE-LCM − Laboratory of Separation and Reaction Engineering - Laboratory of Catalysis and Materials, Faculty of Engineering and ALiCE − Associate Laboratory in Chemical Engineering, Faculty of Engineering, University of Porto, 4200-465 Porto, Portugal;* orcid.org/0000-0002-6746-8973

Complete contact information is available at: https://pubs.acs.org/10.1021/acs.jced.4c00193

Notes

The authors declare no competing financial interest.

ACKNOWLEDGMENTS

This work was supported by national funds through FCT/MCTES (PIDDAC): LSRE-LCM, UIDB/50020/2020 (DOI: 10.54499/UIDB/50020/2020), and UIDP/50020/2020 (DOI: 10.54499/UIDP/50020/2020) and ALiCE, LA/P/0045/2020 (DOI: 10.54499/LA/P/0045/2020).

NOMENCLATURE

C_b	Liquid phase concentration, g·L^{-1}
C_e	Equilibrium liquid phase concentration, g·L^{-1}
C_0	Initial liquid phase concentration, g·L^{-1}
C^F	Feed concentration, g·L^{-1}
D_{ax}	Axial dispersion coefficient, m^2·s^{-1}
D_m	Molecular diffusivity, m^2·s^{-1}
D_p	Pore diffusion, m^2·s^{-1}
f_h	Dry particle to wet particle ratio, g$_{\text{dry resin}}$·g$^{-1}_{\text{wet resin}}$
K_{L1}	Langmuir equilibrium constant in site 1, L·g^{-1}
K_{L2}	Langmuir equilibrium constant in site 2, L·g^{-1}
k_h	LDF mass transfer coefficient, s^{-1}

https://doi.org/10.1021/acs.jced.4c00193
J. Chem. Eng. Data 2024, 69, 3660−3667

L Column length, m
m_{ads} Dry adsorbent mass, $g_{dry\ resin}$
Pe Peclet number
Q Flow rate, $mL{\cdot}min^{-1}$
$\overline{q}$ Average adsorbed phase concentration, $g{\cdot}g^{-1}_{dry\ resin}$
q_e Equilibrium adsorbed phase concentration, $g{\cdot}g^{-1}_{dry\ resin}$
q^* Experimental adsorbed phase concentration, $g{\cdot}g^{-1}_{dry\ resin}$
Q_{m1} Maximum adsorption capacity in site 1, $g{\cdot}g^{-1}_{dry\ resin}$
Q_{m2} Maximum adsorption capacity in site 2, $g{\cdot}g^{-1}_{dry\ resin}$
R_p Particle radius, m
t Time, s
t_{st} Stoichiometric time, s
u Interstitial velocity, $m^2{\cdot}s^{-1}$
V Solution volume, L
V_c Column volume, L
Z Axial position, m

GREEK LETTERS

ε_b Bulk porosity
ε_p Particle porosity
ρ_p Wet particle density, $g_{wet\ resin}{\cdot}L^{-1}_{wet\ resin}$

SUBSCRIPTS

i Species in the ternary mixture

REFERENCES

(1) Fernández-Rodríguez, J.; Erdocia, X.; Sánchez, C.; González Alriols, M.; Labidi, J. Lignin depolymerization for phenolic monomers production by sustainable processes. *J. Energy Chem.* **2017**, *26* (4), 622−631.
(2) Costa, C. A. E.; Vega-Aguilar, C. A.; Rodrigues, A. E. Added-value chemicals from lignin oxidation. *Molecules* **2021**, *26* (15), 4602.
(3) Costa, C. A. E.; Pinto, P. C. R.; Rodrigues, A. E. Radar tool for lignin classification on the perspective of its valorization. *Ind. Eng. Chem. Res.* **2015**, *54* (31), 7580−7590.
(4) Abdelaziz, O. Y.; Clemmensen, I.; Meier, S.; Costa, C. A. E.; Rodrigues, A. E.; Hulteberg, C. P.; Riisager, A. On the oxidative valorization of lignin to high-value chemicals: A critical review of opportunities and challenges. *ChemSusChem* **2022**, *15* (20), No. e202201232.
(5) Cao, H.; Ji, Y.; Zhou, J.; Zhuang, W.; Niu, H.; Gao, N.; Chen, Y.; Liu, D.; Zhu, C.; Chen, X.; Ying, H.; Wu, J. Competitive adsorption of vanillin and syringaldehyde on a macro-mesopore polymeric resin: modeling. *Bioprocess Biosyst. Eng.* **2019**, *42* (9), 1435−1445.
(6) Soto, M. L.; Moure, A.; Domínguez, H.; Parajó, J. C. Recovery, concentration and purification of phenolic compounds by adsorption: A review. *J. Food Eng.* **2011**, *105* (1), 1−27.
(7) Mota, I. F.; Pinto, P. R.; Loureiro, J. M.; Rodrigues, A. E. Purification of syringaldehyde and vanillin from an oxidized industrial kraft liquor by chromatographic processes. *Sep. Purif. Technol.* **2020**, *234*, 116083.
(8) Toppel, O. Method for the separation of carbonyl compounds. US 2897238A, 1959.
(9) Mota, M. I. F.; Pinto, P. C. R.; Loureiro, J. M.; Rodrigues, A. E. Adsorption of vanillin and syringaldehyde onto a macroporous polymeric resin. *Chem. Eng. J.* **2016**, *288*, 869−879.
(10) Zabkova, M.; Otero, M.; Minceva, M.; Zabka, M.; Rodrigues, A. E. Separation of synthetic vanillin at different pH onto polymeric adsorbent Sephabeads SP206. *Chemical Engineering and Processing: Process Intensification* **2006**, *45* (7), 598−607.
(11) Samah, R. A.; Zainol, N.; Yee, P. L.; Pawing, C. M.; Abd-Aziz, S. Adsorption of vanillin using macroporous resin H103. *Adsorption Science & Technology* **2013**, *31* (7), 599−610.
(12) Gomes, E. D.; Rodrigues, A. E. Lignin biorefinery: Separation of vanillin, vanillic acid and acetovanillone by adsorption. *Sep. Purif. Technol.* **2019**, *216*, 92−101.
(13) Thomas, W. J.; Crittenden, B. *Adsorption Technology and Design*; Butterworth-Heinemann: Oxford, 1998.
(14) Wu, Z.; Jiang, Y.; Wang, X.; Xu, J.; Hu, L. A review on the separation of lignin depolymerized products. *Biomass Conversion and Biorefinery* **2023**, *13*, 16667.
(15) Caetano, M.; Valderrama, C.; Farran, A.; Cortina, J. L. Phenol removal from aqueous solution by adsorption and ion exchange mechanisms onto polymeric resins. *J. Colloid Interface Sci.* **2009**, *338* (2), 402−409.
(16) Agbovi, H. K.; Wilson, L. D. 1 - Adsorption processes in biopolymer systems: fundamentals to practical applications. In *Natural Polymers-Based Green Adsorbents for Water Treatment*; Kalia, S., Ed.; Elsevier, 2021; pp 1−51.
(17) Qiu, N.; Guo, S.; Chang, Y. Study upon kinetic process of apple juice adsorption de-coloration by using adsorbent resin. *J. Food Eng.* **2007**, *81* (1), 243−249.
(18) Mota, M. Fractionation and purification of syringaldehyde and vanilin from oxidation of lignin. *Ph.D. Dissertation*, 2017.
(19) Pinto, P. C. R.; da Silva, E. A. B.; Rodrigues, A. E. Comparative Study of Solid-Phase Extraction and Liquid−Liquid Extraction for the Reliable Quantification of High Value Added Compounds from Oxidation Processes of Wood-Derived Lignin. *Ind. Eng. Chem. Res.* **2010**, *49* (23), 12311−12318.
(20) Poling, B. E.; Prausnitz, J. M.; O'Connell, J. P. *Properties of Gases and Liquids*, 5th ed.; McGraw-Hill Education: New York, 2001.
(21) Wilke, C. R.; Chang, P. Correlation of diffusion coefficients in dilute solutions. *AIChE J.* **1955**, *1* (2), 264−270.
(22) Mota, M. I. F.; Barbosa, S.; Pinto, P. C. R.; Ribeiro, A. M.; Ferreira, A.; Loureiro, J. M.; Rodrigues, A. E. Adsorption of vanillic and syringic acids onto a macroporous polymeric resin and recovery with ethanol:water (90:10%V/V) solution. *Sep. Purif. Technol.* **2019**, *217*, 108−117.
(23) Zhang, Q.-F.; Jiang, Z.-T.; Gao, H.-J.; Li, R. Recovery of vanillin from aqueous solutions using macroporous adsorption resins. *European Food Research and Technology* **2008**, *226* (3), 377−383.
(24) Michailof, C.; Stavropoulos, G. G.; Panayiotou, C. Enhanced adsorption of phenolic compounds, commonly encountered in olive mill wastewaters, on olive husk derived activated carbons. *Bioresour. Technol.* **2008**, *99* (14), 6400−6408.

https://doi.org/10.1021/acs.jced.4c00193
J. Chem. Eng. Data 2024, 69, 3660−3667